

1 **Forward genetic screen for *Caenorhabditis elegans* mutants with a shortened**
2 **locomotor healthspan**

3
4 Kazuto Kawamura^{a1} and Ichiro N. Maruyama^{a1}

5
6 ^aInformation Processing Biology Unit, Okinawa Institute of Science and Technology
7 Graduate University, 1919-1 Tancha, Onna-son, Kunigami-gun, Okinawa, Japan, 904-
8 0495

9
10 ¹To whom correspondence may be addressed. Email: kazuto.kawamura@oist.jp or
11 ichi@oist.jp

12
13 Short Title: Shortened locomotor healthspan

14
15 Keywords: *elpc-2*, age-related locomotor impairment, forward genetic screen

17 **Abstract:** Two people with the same lifespan do not necessarily have the same
18 healthspan. One person may retain locomotor and cognitive functions until the end of life,
19 while another person may lose them during adulthood. Unbiased searches for genes that
20 are required to maintain locomotor capacities during adulthood may uncover key
21 regulators of locomotor healthspan. Here, we take advantage of the relatively short
22 lifespan of the nematode *Caenorhabditis elegans* and develop a novel screening
23 procedure to collect mutants with locomotor deficits that become apparent in adulthood.
24 After ethyl methanesulfonate mutagenesis, we isolated five *C. elegans* mutant strains that
25 progressively lose adult locomotor activity. In one of the mutant strains, a nonsense
26 mutation in Elongator Complex Protein Component 2 (*elpc-2*) causes a progressive
27 decline in locomotor function. Mutants and mutations identified in the present screen may
28 provide insights into mechanisms of age-related locomotor impairment and the
29 maintenance of locomotor healthspan.
30

31 **Introduction**

32 Locomotor ability indicates an animal's healthspan across many species such as
33 worms, flies, mice, and humans (Cesari et al., 2009; Grotewiel et al., 2005; Hahm et al.,
34 2015; Justice et al., 2014). In these species, declines in locomotor capacities can be a
35 feature of the normal aging process, or a symptom of an age-related disease. Currently,
36 the genetic regulators that work to prevent age-related declines in locomotor function is
37 largely unknown.

38 Recent studies have suggested that the genetic bases of lifespan and healthspan
39 may not completely overlap (Bansal et al., 2015; Iwasa et al., 2010; Tissenbaum, 2012).
40 From a candidate-based genetic screen, Iwasa *et al.* found that activation of the epidermal
41 growth factor signaling pathway prolongs adult swimming ability in *C. elegans* without
42 large effects on lifespan (Iwasa et al., 2010). More examples of genetic pathways that
43 work to maintain locomotor healthspan may be discovered by carrying out unbiased
44 searches for mutant animals that show progressive declines in locomotor capacity.

45 A forward genetic screen using *C. elegans* has previously been employed to
46 identify genes that affect locomotor function during development (Brenner, 1974).
47 However, unbiased screens that focus on locomotor deficits occurring later in life have
48 not been carried out, in part due to the difficulty in distinguishing whether symptoms
49 observed during adulthood were already present during development.

50 In the present study, we established the "Edge Assay" to measure locomotor
51 ability of hundreds of adult worms at once. Using the Edge Assay, we developed a
52 screening procedure to remove mutant worms with strong developmental locomotor
53 defects on the first day of adulthood, and then isolated mutant worms that progressively
54 lose their locomotor function on the third or fifth days of adulthood. After ethyl
55 methanesulfonate-mutagenesis, we isolated five mutant strains that progressively lose
56 their ability to complete the Edge Assay. In one mutant strain, we found that a mutation
57 in the *elpc-2* gene causes progressive loss of locomotor function. *elpc-2* works with
58 other Elongator complex genes, *elpc-1* and *elpc-3*, to maintain adult locomotor function
59 in *C. elegans*. Along with the Elongator complex mutants, isolated mutants from our
60 screen can be used as tools to explore mechanisms that work to maintain adult
61 locomotor function in *C. elegans*.

62

63 **Results**

64 **The "Edge Assay" can test locomotor function of hundreds of worms**

65 Our forward genetic screen isolates mutant worms that progressively lose
66 locomotor function. We established the Edge Assay to measure locomotor activity of
67 hundreds of worms at once. The Edge Assay is carried out on a 9-cm agar plate with *E.*
68 *coli* bacterial feed spread only on the outer edge of the plate. Up to a few hundred adult
69 worms are placed on the center of the plate where there is no food (Fig. 1A; Fig. S1).

70 Motile worms reach the *E. coli* on the edge of the plate, while worms with defects in
71 locomotion or chemotaxis remain in the center of the plate.

72 On the first day of adulthood, 91.3% of wild-type worms reached the edge in 15
73 min and 99.6% reached the edge in 60 min (Fig. 1B; Fig. S1). *C. elegans* mutant strains
74 that are defective in the function of neurons (*unc-13(e51)*, *unc-43(e408)*) (Maruyama and
75 Brenner, 1991; Reiner et al., 1999) or muscles (*unc-54(e190)*) (MacLeod et al., 1981)
76 could not reach the edge in 15 min on the first day of adulthood (Fig. 1C). After 60 min,
77 26% of *unc-54(e190)* mutants, 6.4% of *unc-43(e408)* mutants, and 0% of *unc-13(e51)*
78 mutants reached the edge (Fig. 1C). Therefore, carrying out the Edge Assay for 15 min
79 on the first day of adulthood can separate wild-type worms from worms with strong
80 developmental locomotor defects.

81 On average, over 90% of wild-type worms could complete the Edge Assay in 60
82 min during the first five days of adulthood (Fig. 1B). A *C. elegans* model of amyotrophic
83 lateral sclerosis (Hsa-sod-1(127X)) (Gidalevitz et al., 2009) showed a significant
84 reduction in Edge Assay completion rate compared to wild-type worms on the fifth day
85 of adulthood (Fig. 1D). Therefore, carrying out the Edge Assay for 60 min on the fifth
86 day of adulthood can separate wild-type worms from worms that progressively lose their
87 locomotor activity.

88

89 **Isolation of mutants that progressively lose locomotor activity during adulthood**

90 We mutagenized wild-type N2 worms using ethyl methanesulfonate, and
91 screened 3352 F2 offspring from 500 F1 worms (1000 genomes) (Table S1). We carried
92 out the Edge Assay for the mutagenized F2 offspring on the first day of adulthood (Fig.
93 2A). To remove worms with developmental defects, worms that could not complete the
94 Edge Assay in 15 min were aspirated away (Fig. 2A). Only worms that completed the
95 Edge Assay on the first day of adulthood were kept for further screening. On the third and
96 fifth days of adulthood, we tested the worms again with the Edge Assay and collected
97 slow or uncoordinated mutants that remained near the center of the Edge Assay plate after
98 60 min (Fig. 2A). By removing worms with strong developmental defects on the first day
99 of adulthood, we were able to isolate worms that progressively lost locomotor function
100 during adulthood. We isolated 22 viable mutants, and created individual strains from
101 those mutants (Table S1). Five of those mutant strains reproducibly showed progressive
102 deficits in completing the Edge Assay during adulthood (Fig. 2B).

103 To determine whether isolated mutant strains have deficits in locomotor function
104 and not sensory function or search behavior, we measured locomotor function of worms
105 on an agar plate without food. We recorded one-minute videos of 15 worms freely moving
106 on a plate, and measured the maximum velocities and total travel distances for each worm.
107 For each strain, we recorded three plates of 15 worms on the first, third, and fifth days of
108 adulthood. All isolated mutant strains showed significantly greater reductions in
109 maximum velocity and travel distance from the first to fifth days of adulthood compared

110 to wild type except for *ix240* worms (Fig. 3A, B, D; Fig. S2A–D; Fig. S3A–D). In the
111 *ix240* worms, progressive deficits other than locomotor function, such as sensory function
112 or search behavior, may cause the reduction in Edge Assay completion rate.

113

114 ***ix241* and *ix243* mutant strains show progressive decline in locomotor function**

115 *ix241* and *ix243* worms were backcrossed with the parental N2 strain to reduce
116 the number of mutation sites that do not affect locomotor function. After each backcross,
117 we checked for individual lines that still showed a progressive decline in locomotor
118 function. We measured the maximum velocity and travel distance of individual worms
119 on an agar plate without food on the first, third, and fifth days of adulthood. *ix241* and
120 *ix243* worms still showed significant reductions in both maximum velocity and travel
121 distance after the fourth backcross (Fig. 3A, B, D; Fig. S3A–D).

122 To check whether *ix241* and *ix243* worms were simply aging faster than wild-
123 type worms, we measured lifespans of the two strains. The lifespan of *ix241* worms was
124 not significantly shortened compared to that of wild type (Fig. 3E; Table S2). The median
125 lifespan of the *ix243* worms was shortened by two days (Fig. 3C; Table S2). To compare
126 relative reductions in lifespan and locomotor healthspan, we measured the maximum
127 velocities of wild type and *ix243* worms for 10 days (Fig. S4A). We quantified the percent
128 decrease in lifespan by comparing the areas under the survival curves of wild type and
129 *ix243* worms (Fig. S4B). We quantified the percent decrease in locomotor healthspan by
130 comparing the areas under the decline in maximum velocity curves of wild type and *ix243*
131 worms (Fig. S4C). For *ix243* worms, there is an average 11.5% reduction in lifespan,
132 while there is a significantly greater 18.5% reduction in locomotor healthspan (Fig. S4D).

133 *ix243* worms take a 13.9% longer time to reach adulthood (Table S3). The
134 developmental delay was taken into account for locomotor and lifespan measurements by
135 allowing *ix243* worms an extra 10 h to develop, and starting locomotor and lifespan
136 measurements from the first day of adulthood. *ix243* worms show a 17.7% decrease in
137 maximum locomotor activity on the first day of adulthood compared to wild-type worms
138 (Fig. 3B). The deficit in locomotor capacity compared to wild-type worms increases to
139 54.8% on the fifth day of adulthood (Fig. 3B). These results suggest that the *ix243* mutant
140 allele has modest negative effects on development and lifespan, with relatively stronger
141 negative effects on locomotor healthspan.

142 *ix241* worms take 4.0% longer to reach adulthood (Table S3) and show an 18.1%
143 decrease in maximum locomotor activity on the first day of adulthood compared to wild-
144 type worms (Fig. 3D). The deficit in locomotor function compared to wild-type worms
145 increases to 43.0% on the fifth day of adulthood (Fig. 3D). The *ix241* mutant allele has
146 no negative effect on lifespan, a modest negative effect on development, and a relatively
147 stronger negative effect on locomotor healthspan.

148

149 **Nonsense mutation in *elpc-2* causes progressive loss of adult locomotor function in**
150 ***ix243* worms**

151 We used whole genome sequencing and a modified version of the sibling
152 subtraction method to identify the causative mutation site in the *ix243* strain (Fig. S5)
153 (Joseph et al., 2018). Mutations were evenly induced on all chromosomes in the *ix243*
154 mutant strain before backcrossing (Fig. 4A). Many mutations remained on Chromosome
155 III after comparing mutations in backcrossed strains that show a progressive loss of
156 adult locomotor function and subtracting mutations in backcrossed strains that do not
157 show progressive loss of adult locomotor function (Fig. 4B; Table S4). A nonsense
158 mutation from TGG to TAG within the protein coding region of *elpc-2* was predicted to
159 disrupt protein function (Fig. 4C; Table S4). Presence of the *elpc-2* mutation site was
160 confirmed by Sanger sequencing (Fig. 4D).

161 To test whether loss of *elpc-2* causes a progressive decline in locomotor
162 function, we injected a genomic fragment of *elpc-2* including 2090-base pairs (bp)
163 upstream of the start codon and 851-bp downstream of the stop codon in the *ix243*
164 mutant strain. The wild-type *elpc-2* fragment rescued the progressive loss of adult
165 locomotor function (Fig. 4E, F; Fig. S6A, B). These results suggest that *elpc-2* is
166 required for maintenance of adult locomotor function in *C. elegans*. The *ix243* mutant
167 strain is the first reported mutant of the *elpc-2* gene in *C. elegans*.

168

169 **The Elongator complex is required to maintain locomotor function**

170 ELPC-2 is a component of the Elongator complex. In *C. elegans*, there are four
171 predicted components of the Elongator complex (ELPC1–4) (Solinger et al., 2010). To
172 test whether functional loss of *elpc-2* causes the locomotor defect independently or as
173 part of the Elongator complex, we measured locomotor activity of strains carrying
174 deletions in *elpc-1* and *elpc-3*. We found that *elpc-1(tm2149)* and *elpc-3(ok2452)*
175 mutant strains also cannot maintain locomotor function during adulthood (Fig. 5A, B).
176 *elpc-1(tm2149);elpc-2(ix243)* and *elpc-2(ix243);elpc-3(ok2452)* double mutants did not
177 show additive deficiencies in locomotor function (Fig. 5C; S7A–H). These results
178 suggest that proper functioning of the entire Elongator complex is necessary to maintain
179 locomotor healthspan. We assessed the expression pattern of *elpc-2* by creating an *elpc-*
180 *2p::GFP* transcriptional reporter that expresses GFP under control of the *elpc-2*
181 promoter. The transcriptional reporter was broadly expressed in many tissues including
182 head and body wall muscles, head neurons, pharynx, canal cell, coelomocytes, intestine,
183 and tail (Fig. S8A–C). The expression pattern of *elpc-2* overlaps with previously
184 reported expression of *elpc-1* in the pharynx, head neurons, and body wall muscles
185 (Chen et al., 2009).

186

187 **Loss-of-function mutation in *tut-1* also causes progressive decline in locomotor**

188 **function**

189 Mutants for *elpc-1* and *elpc-3* have previously been reported to modify the
190 wobble uridine (U₃₄) of tRNA by adding carbamoylmethyl (ncm) and
191 methoxycarbonylmethyl (mcm) side chains to the 5' carbon of U₃₄ (Chen et al., 2009;
192 Nedialkova and Leidel, 2015). Wobble uridines with the mcm⁵ modification are further
193 modified by TUT-1 to add a thio-group at the 2' carbon to create mcm⁵s²U (Chen et al.,
194 2009). In wild-type worms, only ncm⁵ and mcm⁵s² modifications are present (Chen et
195 al., 2009). In *tut-1(tm1297)* mutants, an mcm⁵ modification was observed, which is not
196 normally present in wild-type worms (Chen et al., 2009). In *elpc* mutants, an s²
197 modification was observed, which is not normally present in wild-type worms (Chen et
198 al., 2009).

199 To check whether loss of tRNA thiolation could cause a progressive decline in
200 locomotor function, we measured the locomotor function of *tut-1(tm1297)* mutant
201 worms. *tut-1(tm1297)* mutant worms showed a significantly greater decline in
202 locomotor function during adulthood compared to wild-type worms, indicating that
203 tRNA modifications may be a general mechanism involved in maintenance of
204 locomotor healthspan in *C. elegans* (Fig. 6A; Fig. S9A, B).

205 The *elpc-2(ix243);tut-1(tm1297)* double mutant showed synthetic effects for
206 locomotor function and for developmental maturation. *elpc-2(ix243);tut-1(tm1297)*
207 double mutant worms showed a strong defect in locomotor function on the first day of
208 adulthood and a significantly greater reduction in maximum velocity and travel distance
209 during adulthood relative to either of the single mutants (Fig. 6A; Fig. S9A, B). In
210 addition, *elpc-2(ix243);tut-1(tm1297)* double mutant worms took almost twice as long
211 to reach adulthood (145.4 h) compared to *elpc-2(ix243)* worms (80.2 h) or *tut-*
212 *1(tm1297)* worms (82.0 h) (Table S3; Table S5). The synthetic effects may be explained
213 by the complete absence of U₃₄ modifications in the *elpc-2(ix243);tut-1(tm1297)* double
214 mutant strain. The presence of the s² modification in the *elpc* mutants, and the presence
215 of the mcm⁵ and ncm⁵ modifications in the *tut-1* mutant may enable partial tRNA
216 functionality and allow relatively proper development and partial capacities to maintain
217 locomotor function (Fig. 6B).

218

219 **Discussion**

220 In this study, we established the Edge Assay to simultaneously measure
221 locomotor function of up to a few hundred adult worms. For our forward genetic screen,
222 we used the Edge Assay to remove worms with strong developmental locomotor defects,
223 and isolated worms with locomotor deficits that become apparent in adulthood. By
224 carrying out the Edge Assay on the first day of adulthood, we were able to remove worms
225 with strong developmental locomotor defects and overcome the difficulty of
226 distinguishing developmental and progressive locomotor deficit mutants.

227 The Edge Assay may be used for a variety of applications involving locomotor

228 function. For example, the Edge Assay can be used in suppressor screens to search for
229 mutant worms that show improvements in locomotor function of previously characterized
230 *C. elegans* models of neurodegenerative disease. It may also be possible to use the Edge
231 Assay to screen for other types of progressive declines in functional capacity such as
232 sensory or cognitive deficits by replacing the food ring with specific chemicals or learned
233 cues.

234 The *ix241* and *ix243* mutant strains show similar declines in locomotor function,
235 but have different phenotypes in regard to lifespan. This suggests that genes that regulate
236 lifespan and locomotor healthspan may not completely overlap. In terms of improving
237 quality of life, genetic regulators of healthspan may be better therapeutic targets than
238 regulators of lifespan. Further studies and genetic screens that focus on healthspan-related
239 phenotypes may provide novel insights into mechanisms that regulate healthspan and
240 quality of life across many species.

241 In the *ix243* mutant strain, we found that *elpc-2* is required to maintain locomotor
242 healthspan, and works as part of the Elongator complex. The Elongator complex is an
243 evolutionarily conserved protein complex that consists of six subunits in *S. cerevisiae*, *A.*
244 *thaliana*, *M. musculus*, and humans (Creppe and Buschbeck, 2011; Dauden et al., 2017).
245 ELP1–ELP3 form the core complex, and ELP4–ELP6 form a sub-complex (Creppe and
246 Buschbeck, 2011). In *C. elegans*, there are currently only four predicted homologs of the
247 Elongator complex (*elpc-1–4*). From the present study, loss-of-function mutations in *elpc-*
248 *1*, *elpc-2*, and *elpc-3* caused a shortened locomotor healthspan. Proper functioning of the
249 Elongator complex may require multiple or all components of the complex (Dauden et
250 al., 2017). The present work suggests that the Elongator complex is essential in
251 maintenance of locomotor healthspan.

252 Allelic variants of ELP3, the catalytic subunit of the Elongator complex, were
253 found to be associated with amyotrophic lateral sclerosis (ALS) in three human
254 populations (Simpson et al., 2009). Risk-associated alleles have lower levels of ELP3 in
255 the cerebellum and motor cortex of ALS patients, and protection-associated alleles have
256 higher levels of ELP3 (Simpson et al., 2009). Overexpression of ELP3 reduced levels of
257 axonopathy in the SOD1^{A4V} zebrafish model of ALS and SOD1^{G93A} mouse model of ALS
258 (Bento-Abreu et al., 2018). The present work complements studies that have been
259 performed in the context of ALS, and suggest that loss of the Elongator complex alone
260 can cause locomotor deficits during adulthood in *C. elegans*. Future therapies that target
261 multiple subunits of the Elongator complex may provide more robust effects than
262 therapies that target only the catalytic ELP3 subunit.

263 ELP2 mutations were reported as the causative mutations in a familial form of
264 neurodevelopmental disability (Cohen et al., 2015). Patients who are compound
265 heterozygotes for two different ELP2 missense mutations demonstrate a lack of motor
266 control starting in early development, severe intellectual disability, and progressive loss
267 of locomotor function (Cohen et al., 2015). In our newly isolated *elpc-2(ix243)* strain, we

268 also see deficits in locomotor function on the first day of adulthood and a delay in
269 development (Fig. 3A, B; Fig. S3A, B; Table S3). Since the amino acid sequences of *C.*
270 *elegans* ELPC-2 and human ELP2 are highly conserved (Fig. S10), some aspects of the
271 neurodevelopmental dysfunctions that result from the human ELP2 mutation may be
272 modeled in our *elpc-2(ix243)* mutant strain.

273 The Elongator complex was originally identified as a transcriptional regulator
274 associated with RNA polymerase II (Otero et al., 1999). However, follow-up studies have
275 found that the main functions of the Elongator complex may involve tRNA modification
276 (Chen et al., 2009; Huang et al., 2005), and tubulin acetylation (Solinger et al., 2010).
277 The tRNA thiolation mutant, *tut-1(tm1297)*, also showed a progressive decline in
278 locomotor function. In yeast, tRNA modifications are important for proper translation and
279 folding of proteins (Nedialkova and Leidel, 2015). tRNA modifications may affect
280 locomotor healthspan by regulating translation efficiency and protein folding.

281 Starting from an unbiased forward genetic screen using *C. elegans*, we have
282 found that mutations in Elongator complex and *tut-1* cause progressive declines in
283 locomotor function during adulthood. Future screening procedures that utilize the Edge
284 Assay, and further analysis of the isolated mutants from the present screen may provide
285 insights into how locomotor function is maintained during adulthood.

286

287 **Methods**

288 **Strains**

289 *C. elegans* Bristol N2 strain was used as wild type. Worms were cultivated on
290 Nematode Growth Media (NGM) agar plates with *E. coli* strain OP50 at 20°C (Brenner,
291 1974). See Supplementary Information Appendix for strains used in the present study.

292

293 **Edge Assay**

294 Edge Assay plates were prepared by pouring 16 mL of NGM agar into a circular 9 cm
295 plate. NGM plates were dried overnight with the lid on at 25°C, then kept at 4°C until
296 use. On the day before the Edge Assay, a total of 100 µL of *E. coli* suspension was
297 spotted on four spots near the edge of the NGM plate. The tip of a 50 mL serological
298 pipette was briefly placed over a flame to smoothen the tip. The NGM plate was placed
299 on an inoculating turntable and the smoothened pipette tip was held against the *E. coli*
300 drop. The plate was slowly rotated while holding the pipette tip still. The plate was
301 rotated 360° to spread the *E. coli* around the edge of the whole plate. Plates were
302 incubated overnight at 25°C and used the next day. Synchronized worms were collected
303 and washed twice with M9 buffer containing 0.1% gelatin. Worms were placed on the
304 center of an Edge Assay plate and excess M9 buffer was removed with the edge of a

305 Kimwipe. The number of worms that reached or did not reach the edge were counted at
306 various time points to measure the Edge Assay completion rate.

307

308 **Isolation of mutants that show a progressive decline in locomotor function**

309 Wild-type N2 worms were mutagenized and cultured as previously described (Brenner,
310 1974). Larval stage 4 worms were mutagenized by incubation in a 50 mM ethyl
311 methanesulfonate solution for 4 h. EMS-mutagenized F2 adult day 1 worms were
312 collected and washed twice with M9 buffer containing 0.1% aqueous gelatin. Worms
313 were placed at the center of an Edge Assay plate and excess buffer was removed with
314 the edge of a Kimwipe. After 15 min, worms that did not reach the edge were removed
315 using an aspirator. Worms that reached the edge were maintained on the same plate
316 until adult day 3. On adult day 3, worms were collected and washed with M9 buffer
317 containing 0.1% gelatin and the Edge Assay was repeated on a new Edge Assay plate.
318 Worms that were unable to reach the edge were collected as adult day 3 progressive
319 locomotor deficit mutants. Worms that reached the edge were maintained on the same
320 plate until adult day 5. On adult day 5, worms were collected and washed with M9
321 buffer containing 0.1% gelatin and the Edge Assay was repeated on a new Edge Assay
322 plate. Worms that were unable to reach the edge were collected as adult day 5
323 progressive locomotor deficit mutants.

324

325 **Measurements of maximum speed and travel distance**

326 Worms were synchronized by placing five adult day 1 worms onto an NGM plate with
327 food, and allowed to lay eggs for 3 h. When the offspring reached adult day 1, 15
328 worms were picked randomly onto a 6 cm NGM plate without bacteria. After the worms
329 moved away from the initial location with residual food, worms were again moved onto
330 a different NGM plate without bacteria. Movement of worms was recorded for 1.0 min
331 with a charge-coupled device camera INFINITY3-6URM (Lumenera Corporation,
332 Ottawa, Canada). Images were analyzed using ImageJ and wrMTrck software
333 (www.phage.dk/plugins) to produce maximum speed and travel distance (Nussbaum-
334 Krammer et al., 2015). Measurements were made with the lid on in a temperature-
335 controlled room set at 20 °C. At least three biological replicate plates of 15 worms each
336 were measured for each strain. Worms that were lost during the video recording were
337 not included in the analysis.

338

339 **Whole-genome DNA sequencing**

340 *C. elegans* DNA was sequenced using the MiSeq platform (Illumina, San Diego, CA).
341 Libraries were prepared with an Illumina TruSeq Library Prep Kit. Mapping was

342 conducted with BWA software (Li and Durbin, 2009). Resulting files were converted to
343 bam files, then to pileup format with Samtools (Li et al., 2009). Variant analysis was
344 conducted using VarScan and SnpEff available on the Galaxy platform (Blankenberg et
345 al., 2010; Cingolani et al., 2012; Giardine et al., 2005; Goecks et al., 2010; Koboldt et
346 al., 2009). Mutation frequencies along the chromosome were calculated and visualized
347 using CloudMap (Minevich et al., 2012).

348

349 **Transcriptional reporter expression**

350 A genomic fragment of 2090-bp immediately upstream of the start codon of the *elpc-2*
351 gene was PCR-amplified using “5' *elpc-2p* overlap ppd95.79 107-” and “3' *elpc-2p*
352 overlap ppd95.79 138-” primers, which have 15-bp overhangs that anneal immediately
353 upstream of the GFP sequence in the pPD95.79 vector (See Supplementary Information
354 for primers used). The pPD95.79 vector containing GFP was linearized by PCR using
355 the “5' ppd95.79 107-” and “3' ppd95.79 138-” primers. The template vector was
356 digested with restriction enzyme *DpnI* (New England Biolabs, Ipswich, MA), and the
357 linearized vector was purified by Wizard SV Gel and PCR Clean-Up System (Promega,
358 Madison, WI). The pure linearized vector and the *elpc-2* promoter were fused using an
359 In-Fusion HD Cloning Kit (Takara, Kusatsu, Japan) to make the *elpc-2p::GFP*
360 transcriptional reporter construct. The construct was microinjected into the gonads of
361 wild-type worms at a concentration of 50 ng/μL. Worms that expressed the reporter
362 construct were immobilized in 25 mM sodium azide and observed under a confocal
363 microscope LSM710 (Carl Zeiss, Oberkochen, Germany). A z-stack image was created
364 from images taken at 1 μm increments.

365

366 **Creation of double mutants**

367 Double mutant strains were created by crossing males of one strain with hermaphrodites
368 of another. Double mutants were checked by extracting their DNA, amplifying a genomic
369 fragment flanking the mutation site by PCR, and sequencing the PCR product by Sanger
370 sequencing. See Supplementary Information for primer details.

371

372 **Statistics**

373 All results are expressed as means with a 95% confidence interval. Student's *t* test was
374 used for pairwise comparisons with Excel 2010 (Microsoft). For multiple comparisons,
375 one-way ANOVA was followed with Dunnett's post hoc test or Tukey's Honest
376 Significant Difference test using R (Team, 2015). Statistical significance was set at **P* <
377 0.05; ***P* < 0.01; ****P* < 0.001.

378

379 **Data availability**

380 All isolated strains and plasmids are available upon request. Whole genome DNA
381 sequencing data is available on NCBI Sequence Read Archive (PRJNA530333
382 SAMN11311296 SAMN11311297).

383

384

385 **Acknowledgements**

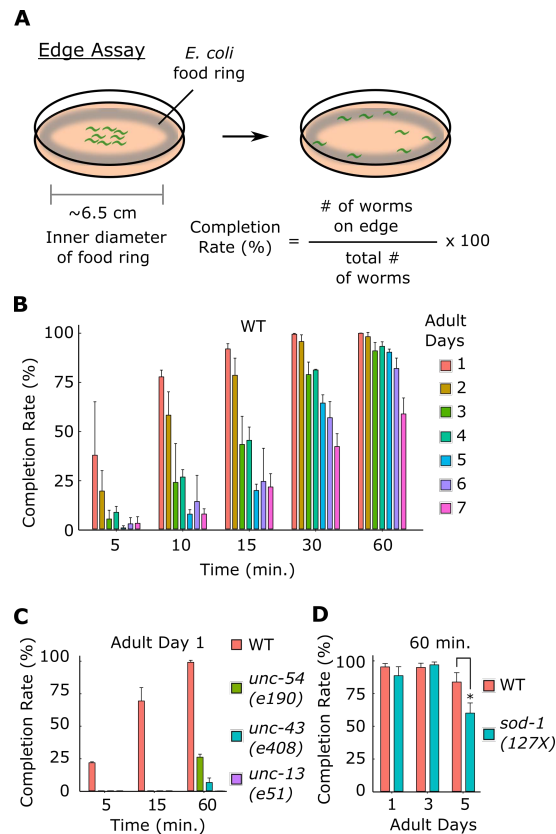
386 We thank H. Goto, M. Kanda, M. Kawamitsu, S. Yamasaki and other DNA sequencing
387 section members for technical assistance with whole genome sequencing. We are grateful
388 to T. Murayama and E. Saita for helpful advice and support. We thank D. Van Vactor, B.
389 Kuhn and members of the Maruyama unit for helpful discussions and comments. We are
390 grateful to H. Ohtaki for administrative support. We thank Steve Aird for technical editing
391 of this manuscript. We thank the *Caenorhabditis* Genetics Center, which is funded by
392 NIH Office of Research Infrastructure Programs (P40 OD010440), for providing worm
393 strains. We also thank the National Bioresource Project (Japan) for providing worm
394 strains. K. K. was supported by Japan Society for the Promotion of Science KAKENHI
(Grant 16J06404).

395 **References**

- 396 Bansal, A., Zhu, L.J., Yen, K., and Tissenbaum, H.A. (2015). Uncoupling lifespan and
397 healthspan in *Caenorhabditis elegans* longevity mutants. Proc. Natl. Acad. Sci. U. S. A.
398 112, E277-286.
- 399 Bento-Abreu, A., Jager, G., Swinnen, B., Rué, L., Hendrickx, S., Jones, A., Staats,
400 K.A., Taes, I., Eykens, C., Nonneman, A., et al. (2018). Elongator subunit 3 (ELP3)
401 modifies ALS through tRNA modification. Hum. Mol. Genet. 27, 1276–1289.
- 402 Blankenberg, D., Kuster, G. Von, Coraor, N., Ananda, G., Lazarus, R., Mangan, M.,
403 Nekrutenko, A., and Taylor, J. (2010). Galaxy: A web-based genome analysis tool for
404 experimentalists. Curr. Protoc. Mol. Biol. 1–21.
- 405 Brenner, S. (1974). *Caenorhabditis elegans*. Genetics 77, 71–94.
- 406 Cesari, M., Pahor, M., Lauretani, F., Zamboni, V., Bandinelli, S., Bernabei, R.,
407 Guralnik, J.M., and Ferrucci, L. (2009). Skeletal muscle and mortality results from the
408 InCHIANTI study. Journals Gerontol. - Ser. A Biol. Sci. Med. Sci. 64, 377–384.
- 409 Chen, C., Tuck, S., and Byström, A.S. (2009). Defects in tRNA Modification
410 Associated with Neurological and Developmental Dysfunctions in *Caenorhabditis*
411 *elegans* Elongator Mutants. PLoS Genet. 5, e1000561.
- 412 Cingolani, P., Platts, A., Wang, L.L., Coon, M., Nguyen, T., Wang, L., Land, S.J., Lu,
413 X., and Ruden, D.M. (2012). A program for annotating and predicting the effects of
414 single nucleotide polymorphisms, SnpEff: SNPs in the genome of *Drosophila*
415 *melanogaster* strain *w* 1118; *iso-2*; *iso-3*. Fly (Austin). 6, 80–92.
- 416 Cohen, J.S., Srivastava, S., Farwell, K.D., Lu, H.M., Zeng, W., Lu, H., Chao, E.C., and
417 Fatemi, A. (2015). ELP2 is a novel gene implicated in neurodevelopmental disabilities.
418 Am. J. Med. Genet. Part A 167, 1391–1395.
- 419 Creppe, C., and Buschbeck, M. (2011). Elongator: an ancestral complex driving
420 transcription and migration through protein acetylation. J. Biomed. Biotechnol. 2011,
421 924898.
- 422 Dauden, M.I., Kosinski, J., Kolaj-Robin, O., Desfosses, A., Ori, A., Faux, C.,
423 Hoffmann, N.A., Onuma, O.F., Breunig, K.D., Beck, M., et al. (2017). Architecture of
424 the yeast Elongator complex. EMBO Rep. 18, 264–279.
- 425 Giardine, B., Riemer, C., Hardison, R.C., Burhans, R., Elnitski, L., Shah, P., Zhang, Y.,
426 Blankenberg, D., Albert, I., Taylor, J., et al. (2005). Galaxy: A platform for interactive
427 large-scale genome analysis. Genome Res. 15, 1451–1455.
- 428 Gidalevitz, T., Krupinski, T., Garcia, S., and Morimoto, R.I. (2009). Destabilizing
429 protein polymorphisms in the genetic background direct phenotypic expression of
430 mutant SOD1 toxicity. PLoS Genet. 5, e1000399.

- 431 Goecks, J., Nekrutenko, A., and Taylor, J. (2010). Galaxy: a comprehensive approach
432 for supporting accessible, reproducible, and transparent computational research in the
433 life sciences. *Genome Biol.* *11*, R86.
- 434 Grotewiel, M.S., Martin, I., Bhandari, P., and Cook-Wiens, E. (2005). Functional
435 senescence in *Drosophila melanogaster*. *Ageing Res. Rev.* *4*, 372–397.
- 436 Hahm, J.-H., Kim, S., DiLoreto, R., Shi, C., Lee, S.-J. V., Murphy, C.T., and Nam, H.G.
437 (2015). *C. elegans* maximum velocity correlates with healthspan and is maintained in
438 worms with an insulin receptor mutation. *Nat. Commun.* *6*, 8919.
- 439 Huang, B., Johansson, M.J.O., and Byström, A.S. (2005). An early step in wobble
440 uridine tRNA modification requires the Elongator complex. *RNA* *11*, 424–436.
- 441 Iwasa, H., Yu, S., Xue, J., and Driscoll, M. (2010). Novel EGF pathway regulators
442 modulate *C. elegans* healthspan and lifespan via EGF receptor, PLC- γ , and IP3R
443 activation. *Aging Cell* *9*, 490–505.
- 444 Joseph, B.B., Blouin, N.A., and Fay, D.S. (2018). Use of a Sibling Subtraction Method
445 for Identifying Causal Mutations in *Caenorhabditis elegans* by Whole-Genome
446 Sequencing. *G3 (Bethesda)*. *8*, 669–678.
- 447 Justice, J.N., Carter, C.S., Beck, H.J., Gioscia-Ryan, R.A., McQueen, M., Enoka, R.M.,
448 and Seals, D.R. (2014). Battery of behavioral tests in mice that models age-associated
449 changes in human motor function. *Age (Omaha)*. *36*, 583–595.
- 450 Koboldt, D.C., Chen, K., Wylie, T., Larson, D.E., McLellan, M.D., Mardis, E.R.,
451 Weinstock, G.M., Wilson, R.K., and Ding, L. (2009). VarScan: Variant detection in
452 massively parallel sequencing of individual and pooled samples. *Bioinformatics* *25*,
453 2283–2285.
- 454 Li, H., and Durbin, R. (2009). Fast and accurate short read alignment with Burrows-
455 Wheeler transform. *Bioinformatics* *25*, 1754–1760.
- 456 Li, H., Handsaker, B., Wysoker, A., Fennell, T., Ruan, J., Homer, N., Marth, G.,
457 Abecasis, G., and Durbin, R. (2009). The Sequence Alignment/Map format and
458 SAMtools. *Bioinformatics* *25*, 2078–2079.
- 459 MacLeod, A., Karn, J., and Brenner, S. (1981). Molecular analysis of the *unc-54*
460 myosin heavy-chain gene of *Caenorhabditis elegans*. *Nature* *291*, 386–390.
- 461 Maruyama, I.N., and Brenner, S. (1991). A phorbol ester/diacylglycerol-binding protein
462 encoded by the *unc-13* gene of *Caenorhabditis elegans*. *Proc. Natl. Acad. Sci.* *88*,
463 5729–5733.
- 464 Minevich, G., Park, D.S., Blankenberg, D., Poole, R.J., and Hobert, O. (2012).
465 CloudMap: a cloud-based pipeline for analysis of mutant genome sequences. *Genetics*
466 *192*, 1249–1269.

- 467 Nedialkova, D.D., and Leidel, S.A. (2015). Optimization of Codon Translation Rates
468 via tRNA Modifications Maintains Proteome Integrity. *Cell* 161, 1606–1618.
- 469 Nussbaum-Krammer, C.I., Neto, M.F., Brielmann, R.M., Pedersen, J.S., and Morimoto,
470 R.I. (2015). Investigating the Spreading and Toxicity of Prion-like Proteins Using the
471 Metazoan Model Organism *C. elegans*. *J. Vis. Exp.* 1–15.
- 472 Otero, G., Fellows, J., Yang, L., De Bizemont, T., Dirac, A.M.G., Gustafsson, C.M.,
473 Erdjument-Bromage, H., Tempst, P., and Svejstrup, J.Q. (1999). Elongator, a
474 multisubunit component of a novel RNA polymerase II holoenzyme for transcriptional
475 elongation. *Mol. Cell* 3, 109–118.
- 476 Reiner, D.J., Newton, E.M., Tian, H., and Thomas, J.H. (1999). Diverse behavioural
477 defects caused by mutations in *Caenorhabditis elegans unc-43* CaM kinase II. *Nature*
478 402, 199–203.
- 479 Sievers, F., Wilm, A., Dineen, D., Gibson, T.J., Karplus, K., Li, W., Lopez, R.,
480 McWilliam, H., Remmert, M., Söding, J., et al. (2011). Fast, scalable generation of
481 high-quality protein multiple sequence alignments using Clustal Omega. *Mol. Syst.*
482 *Biol.* 7.
- 483 Simpson, C.L., Lemmens, R., Miskiewicz, K., Broom, W.J., Hansen, V.K., van Vught,
484 P.W.J., Landers, J.E., Sapp, P., Van Den Bosch, L., Knight, J., et al. (2009). Variants of
485 the elongator protein 3 (ELP3) gene are associated with motor neuron degeneration.
486 *Hum. Mol. Genet.* 18, 472–481.
- 487 Solinger, J.A., Paolinelli, R., Klöß, H., Scorza, F.B., Marchesi, S., Sauder, U.,
488 Mitsushima, D., Capuani, F., Stürzenbaum, S.R., and Cassata, G. (2010). The
489 *Caenorhabditis elegans* Elongator Complex Regulates Neuronal α -tubulin Acetylation.
490 *PLoS Genet.* 6, e1000820.
- 491 Team, R.C. (2015). R: A language and environment for statistical computing [Internet].
492 Vienna, Austria: R Foundation for Statistical Computing; 2015.
- 493 Tissenbaum, H.A. (2012). Genetics, Life span, Health Span, and the Aging Process in
494 *Caenorhabditis elegans*. *J. Gerontol. A. Biol. Sci. Med. Sci.* 67, 503–510.
- 495

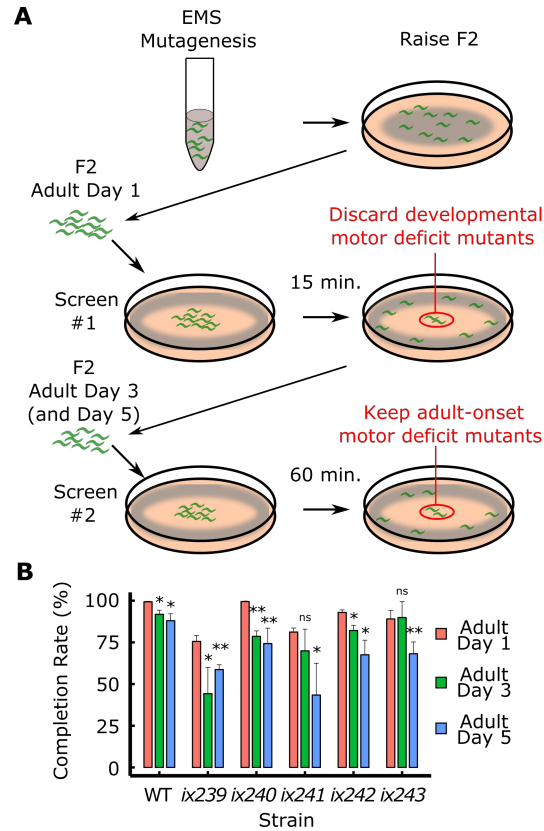


496

497 **Figure 1. “Edge Assay” can measure locomotor ability of worms**

498 (A) (*Left*) Schematic diagram of an Edge Assay plate immediately after placing worms at
 499 the center of the plate. (*Right*) Schematic diagram of Edge Assay plate after most worms
 500 reached the edge. (B) Edge Assay completion rates of wild-type worms from adult day 1
 501 to 7 after 5, 10, 15, 30, and 60 min. (C) Completion rates for WT and developmental
 502 mutants deficient in locomotor function, *unc-54(e190)*, *unc-43(e408)*, and (*unc-13(e51)*).
 503 (D) Completion rates of WT and a previously reported *C. elegans* model of amyotrophic
 504 lateral sclerosis (Hsa-*sod-1(127X)*). For Edge Assay experiments, n = 3 biological
 505 replicate plates with each plate starting with approximately 100 worms per plate on adult
 506 day 1. Error bars indicate 95% confidence intervals. **P* < 0.05; Unpaired Student’s *t* test
 507 for D.

508

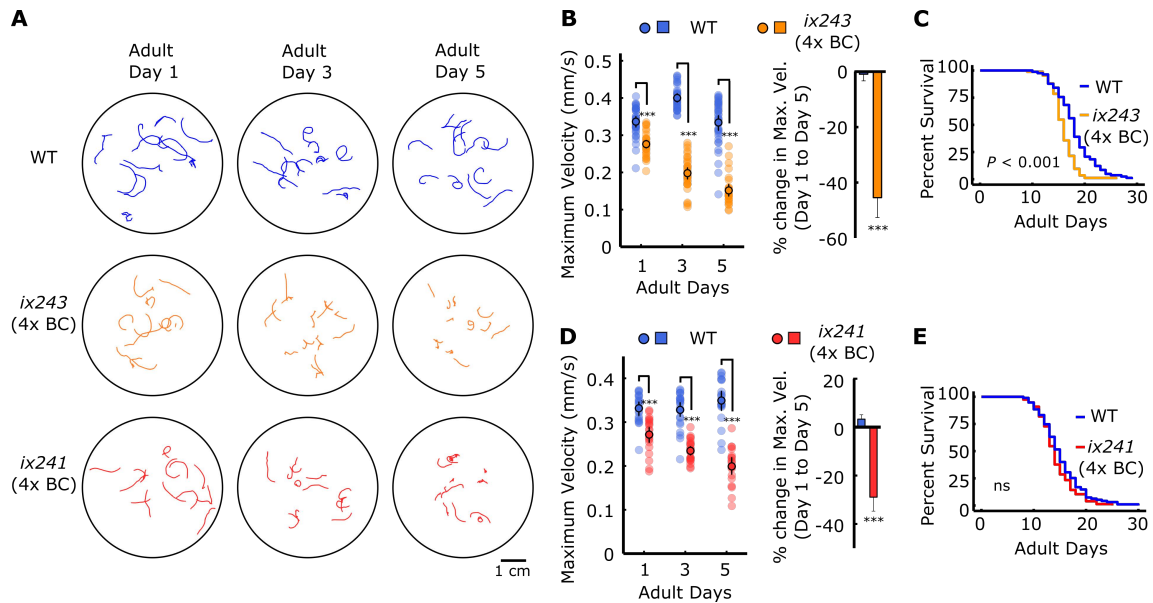


509

510 **Figure 2. Isolation of mutant strains that progressively lose locomotor ability**

511 (A) Schematic description of a forward genetic screen to isolate mutants that
512 progressively lose locomotor ability. (B) Edge Assay completion rates of mutants
513 identified from the screen. Error bars indicate 95% confidence intervals. n = 3 biological
514 replicate plates, with each plate starting with approximately one hundred worms per plate
515 on adult day 1. * $P < 0.05$; ** $P < 0.01$; ns, not significant; Paired Student's t test vs. adult
516 day 1 completion rate.

517

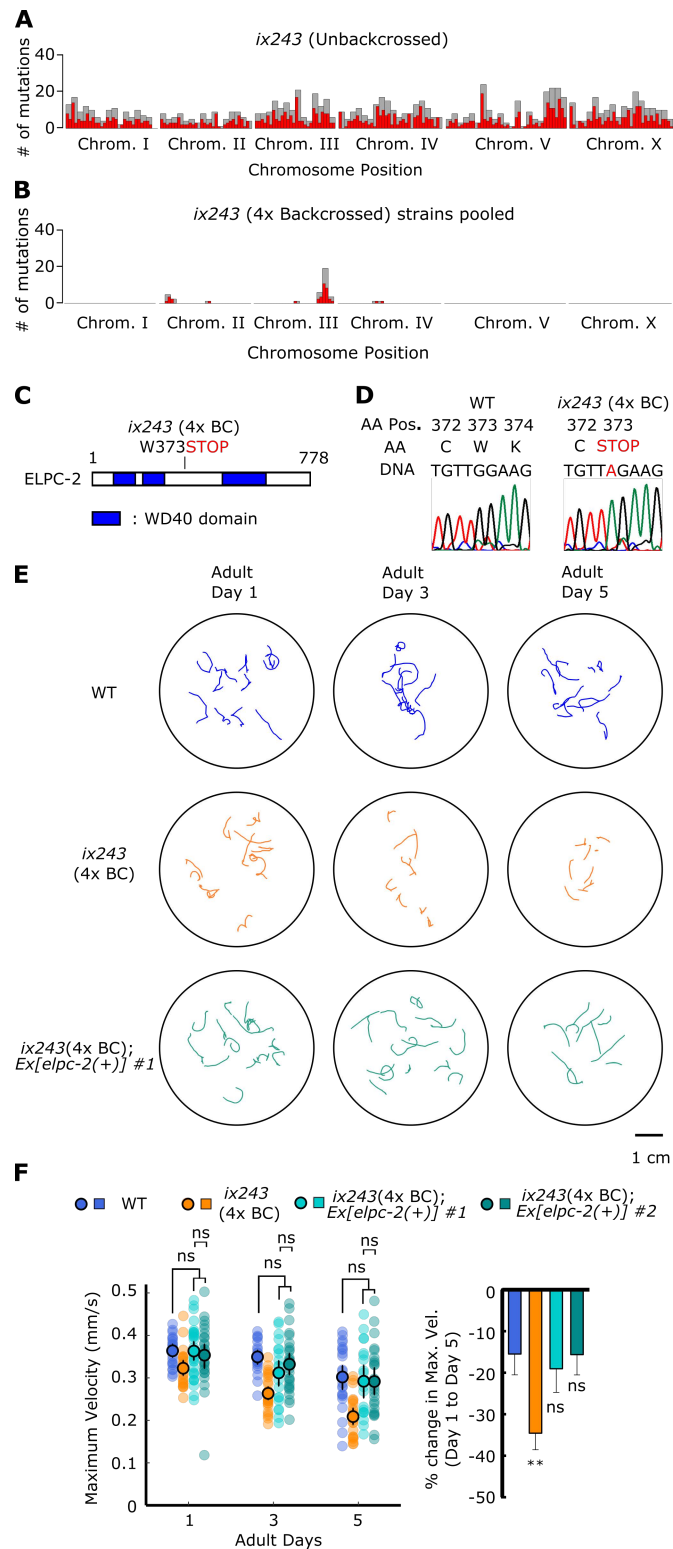


518

519 **Figure 3. *ix241* and *ix243* worms show progressive locomotor decline after four**
 520 **backcrosses**

521 (A) Representative locomotor tracks from 1-min video recordings of wild-type (WT),
 522 *ix243*(backcrossed four times (4x BC)), and *ix241*(4x BC) worms on adult days 1, 3, and
 523 5 on plates with no food. n = 10–15 tracks per plate (some worms were unable to be
 524 tracked for a full minute, and were removed from analysis) (B) (Left) Maximum velocities
 525 of WT and *ix243*(4x BC) worms. (Right) Percent change in maximum velocity of WT and
 526 *ix243*(4x BC) worms on adult day 5 compared to adult day 1. (C) Survival curve of WT
 527 (n = 56 worms) and *ix243*(4x BC) (n = 89) worms.(D) (Left) Maximum velocities of WT
 528 and *ix241*(4x BC) worms. (Right) Change in maximum velocity of WT and *ix241*(4x BC)
 529 worms. (E) Survival curve of WT (n = 94) and *ix241*(4x BC) (n = 77) worms. Error bars
 530 indicate 95% confidence intervals. For maximum velocity experiments, n = 30–45 worms
 531 per strain for each day (10–15 worms from 3 biological replicate plates). For percent
 532 change in maximum velocity graphs, n = 3 biological replicate plates. *** $P < 0.001$; ns,
 533 not significant; Unpaired Student's *t* test for maximum velocity comparisons; Log-rank
 534 test for lifespan comparisons.

535



536

537 **Figure 4. *elpc-2* mutation causes locomotor deficits in the *ix243* mutant strain**

538 (A) Mutation frequency along each chromosome of *ix243* mutant strain before

539 backcrossing. Red bars indicate 0.5-Mb bins and grey bars indicate 1.0-Mb bins. (B)

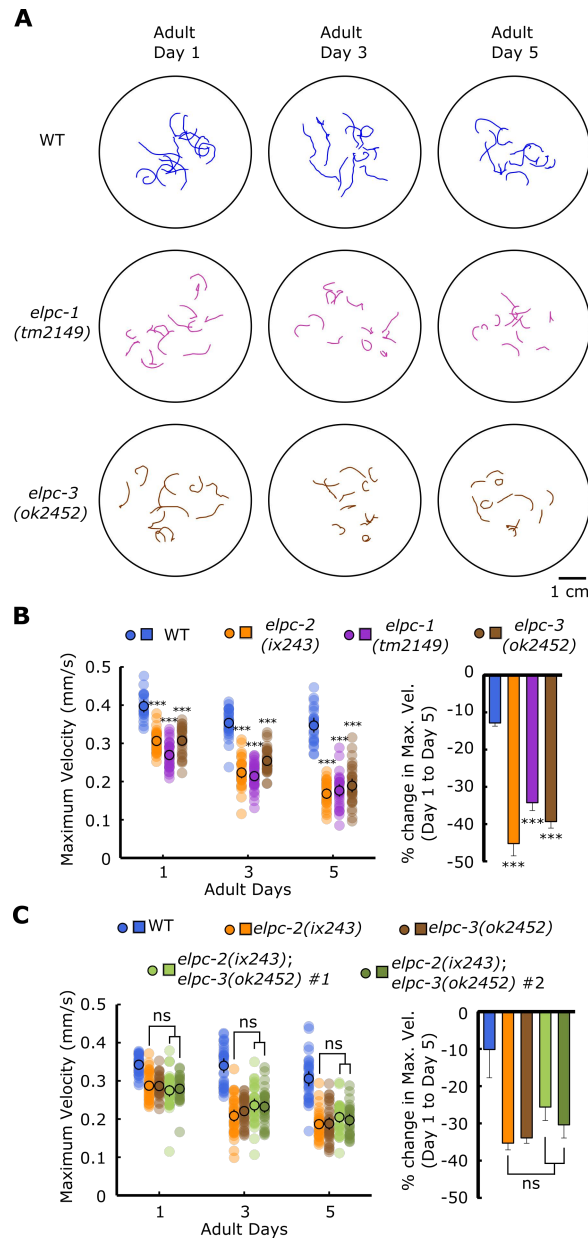
540 Mutation frequency along each chromosome for pooled *ix243*(4x BC) worms. (C)

541 Schematic diagram of ELPC-2 protein and location of mutation site in *ix243* allele. (D)

542 *ix243* mutation site on ELPC-2 amino acid (AA) sequence and *elpc-2* DNA sequence. (E)

543 Representative locomotor tracks of WT, *ix243*(4x BC), and *ix243*(4x BC);*Ex[elpc-2(+)]*

544 #1 worms. (F) (*Left*) Maximum velocities of WT, *ix243*(4x BC), *ix243*(4x BC);*Ex[elpc-*
545 *2(+)]* #1, and *ix243*(4x BC);*Ex[elpc-2(+)]* #2 worms. n = 30–45 worms per strain for
546 each day (10–15 worms from 3 biological replicate plates). (*Right*) Percent change in
547 maximum velocity of worms from left panel. n = 3 biological replicate plates. Error bars
548 indicate 95% confidence intervals. ***P* < 0.01; ns, not significant ; One-way ANOVA
549 with Dunnett’s post hoc test vs. WT.
550



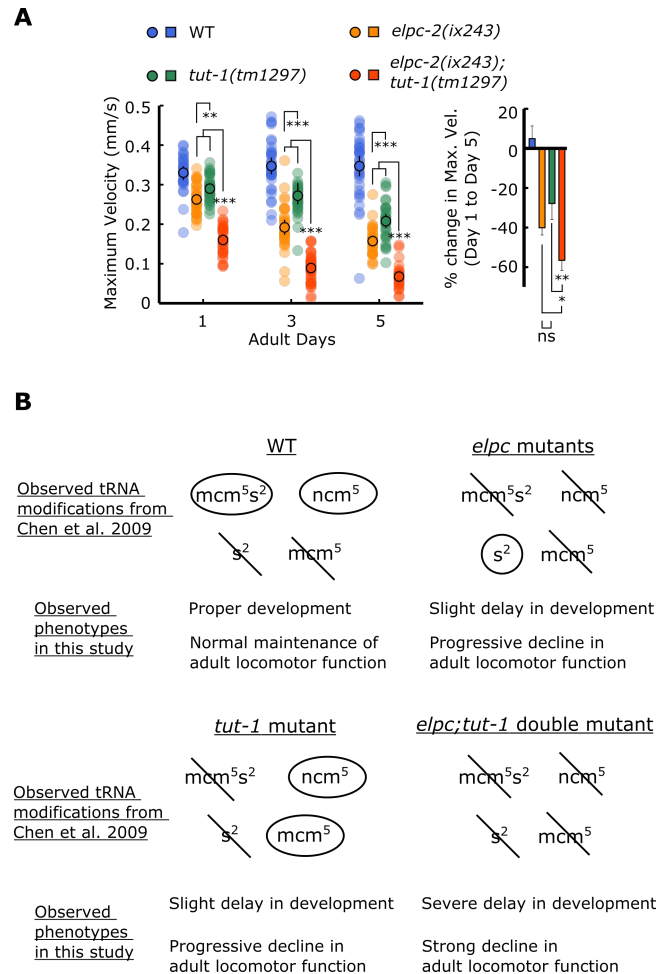
551

552 **Figure 5. The Elongator complex is required to maintain locomotor function**

553 (A) Representative locomotor tracks of WT, *elpc-1*(*tm2149*) and *elpc-3*(*ok2452*) worms.
 554 n = 10–15 tracks per plate. (B) (Left) Maximum velocities of WT *elpc-1*(*tm2149*) and
 555 *elpc-3*(*ok2452*) worms. (Right) Percent change in maximum velocity of worms from left
 556 panel. (C) (Left) Maximum velocities of WT, *elpc-2*(*ix243*), *elpc-3*(*ok2452*), and *elpc-*
 557 *2*(*ix243*);*elpc-3*(*ok2452*) worms. (Right) Percent change in maximum velocity of worms
 558 from left panel. Error bars indicate 95% confidence intervals. For maximum velocity
 559 experiments, n = 30–45 worms per strain for each day (10–15 worms from 3 biological
 560 replicate plates). For percent change in maximum velocity graphs, n = 3 biological
 561 replicate plates. ****P* < 0.001; ns, not significant; One-way ANOVA with Dunnett’s post
 562 hoc test vs. WT for B; One-way ANOVA with Tukey’s post hoc test for C.

563

564



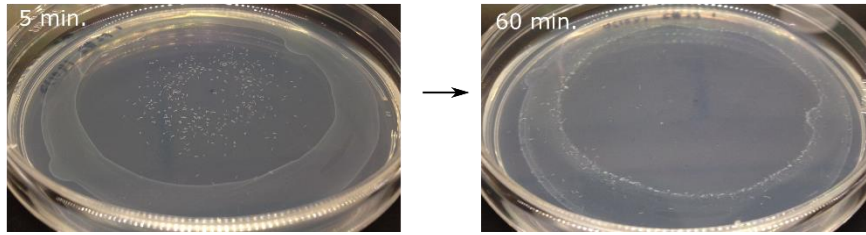
565

566 **Figure 6. *tut-1(tm1297)* mutant shows progressive decline in locomotor function**

567 (A) (Left) Maximum velocities of WT, *elpc-2(ix243)*, *tut-1(tm1297)*, and *elpc-*
568 *2(ix243);tut-1(tm1297)* worms. (Right) Percent change in maximum velocity of worms
569 from left panel. Error bars indicate 95% confidence intervals. n = 30–45 worms per strain
570 for each day (10–15 worms from 3 biological replicate plates). For percent change in
571 maximum velocity graphs, n = 3 biological replicate plates. **P* < 0.05; ****P* < 0.001; ns,
572 not significant; One-way ANOVA with Tukey’s post hoc test. (B) Summary of observed
573 tRNA modifications in *elpc* and *tut-1* mutants from Chen et al. 2009, and summary of
574 observed phenotypes in *elpc* and *tut-1* mutants from this study.

575

576



577

578 **Figure S1. Photos of Edge Assay**

579 (*Left*) Photo of Edge Assay after 5 min with worms moving away from the center. (*Right*)

580 Photo of Edge Assay after 60 min with worms reaching and remaining in the edge.

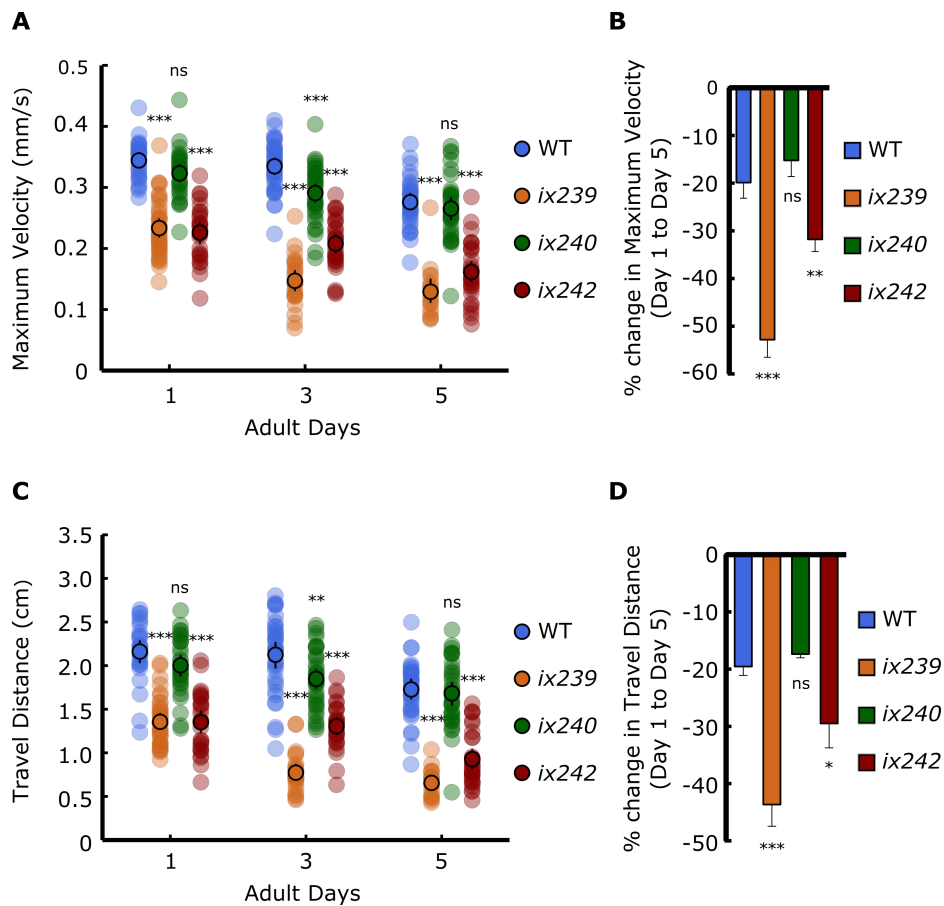
581

582 **Table S1. Number of screened genomes and isolated mutants**

	EMS-mutagenesis I			EMS-mutagenesis II			Total
	Day 1	Day 3	Day 5	Day 1	Day 3	Day 5	
Genomes Screened	400			600			
Isolated mutants		13	23		17	17	70
Viable isolated mutants		3	8		9	2	22
Isolated mutants with reproducible deficits		0	3		2	0	5

583

584

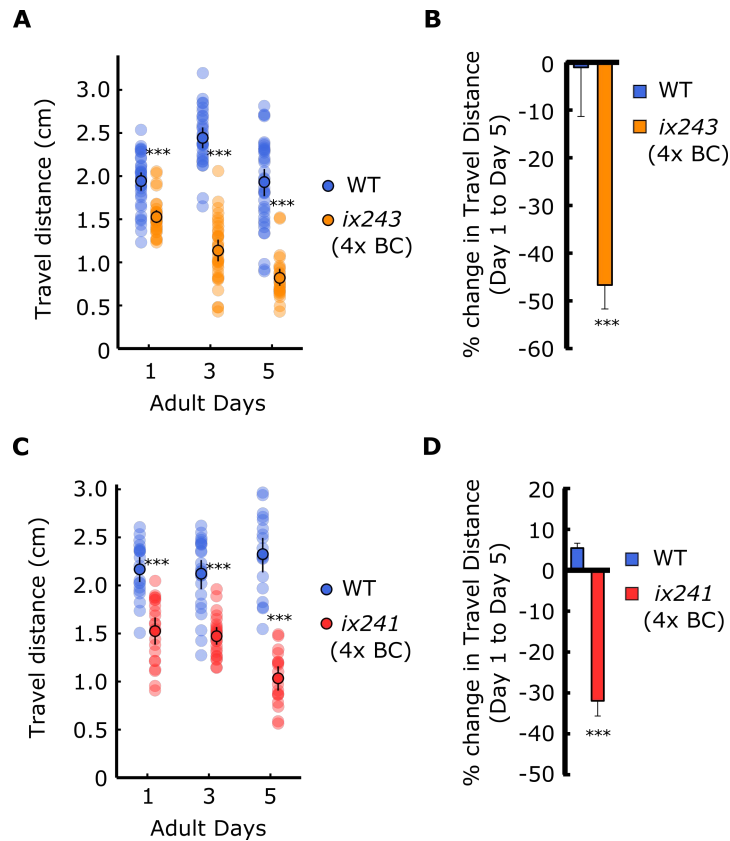


585

586 **Figure S2. Maximum velocity and travel distance of isolated mutants**

587 (A) Maximum velocities of WT, *ix239*, *ix240*, and *ix242* worms. (B) Percent change in
588 maximum velocity of worms from A. (C) Travel distances of WT, *ix239*, *ix240*, and *ix242*
589 worms. (D) Percent change in travel distance of worms from C. Error bars indicate 95%
590 confidence intervals. For maximum velocity and travel distance experiments, $n = 30-45$
591 worms per strain for each day (10–15 worms from 3 biological replicate plates). For
592 percent change in maximum velocity graphs, $n = 3$ biological replicate plates. $*P < 0.05$;
593 $**P < 0.01$; $***P < 0.001$; ns, not significant; One-way ANOVA with Dunnett's post hoc
594 test vs. WT.

595



596

597 **Figure S3. *ix241* and *ix243* worms show progressive locomotor decline after four**
598 **backcrosses**

599 (A) Travel distances of WT and *ix243* worms (backcrossed four times (4x BC)). (B)
600 Percent change in travel distance of WT and *ix243*(4x BC) worms. (C) Travel distances
601 of WT and *ix241*(4x BC) worms. (D) Percent change in travel distance of WT and
602 *ix241*(4x BC) worms. For travel distance experiments, n = 30–45 worms per strain for
603 each day (10–15 worms from 3 biological replicate plates). For percent change in travel
604 distance graphs, n = 3 biological replicate plates. *** $P < 0.001$; Unpaired Student's *t* test
605 vs. WT.

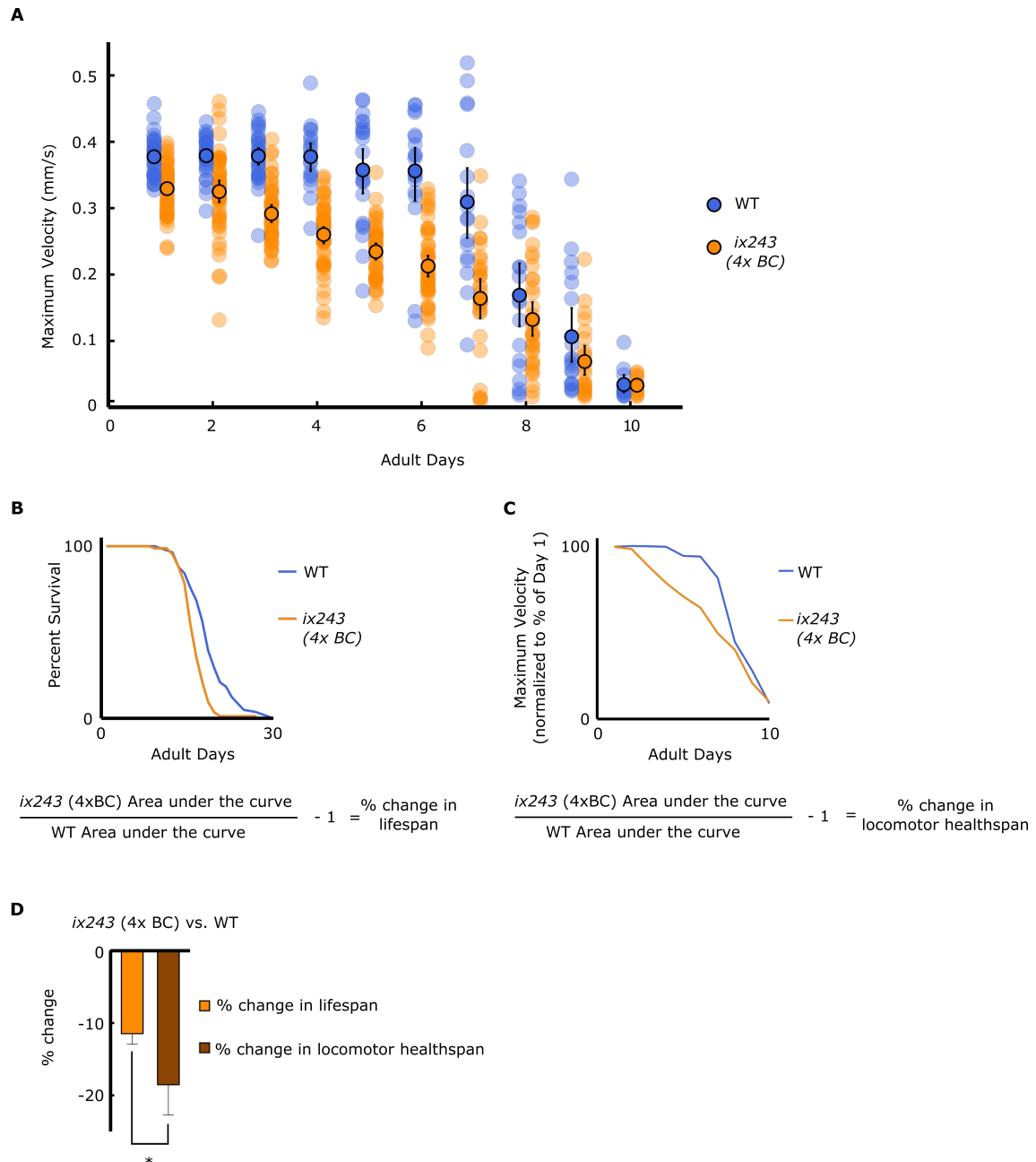
606

607 **Table S2. Lifespan Analysis**

Strain	Median Lifespan (adult days)	<i>P</i> value vs WT (Log-rank test)	Worms (Counted/Total)	FUDR
N2	18		56/90	25 µg/ml
<i>ix243</i> (4x backcrossed)	16	<i>P</i> = 0.00078	89/90	25 µg/ml
N2	18		82/90	25 µg/ml
<i>ix243</i> (4x backcrossed)	16	<i>P</i> < 0.0001	84/90	25 µg/ml
N2	18		87/90	25 µg/ml
<i>ix243</i> (4x backcrossed)	16	<i>P</i> < 0.0001	87/90	25 µg/ml
N2	17		94/120	0
<i>ix241</i> (4x backcrossed)	16	<i>P</i> = 0.095	77/120	0
N2	14		66/90	0
<i>ix241</i> (4x backcrossed)	15	<i>P</i> = 0.12	64/90	0
N2	12		67/90	0
<i>ix241</i> (4x backcrossed)	14	<i>P</i> = 0.024	74/90	0

608

609



610

611 **Figure S4. Greater reduction in total locomotor healthspan compared to lifespan in**
 612 ***ix243* worms**

613 (A) Maximum velocities of WT and *ix243* (4x backcrossed (4x BC)) worms. n = 30–45
 614 worms per strain for each day (10–15 worms from 3 biological replicate plates). (B)
 615 (Top) Representative survival curve of WT (n = 56 worms) and *ix243*(4x BC) worms (n
 616 = 89 worms). (Bottom) Calculation method of percent change in lifespan. (C) (Top)
 617 Representative decline in maximum velocity curve of WT and *ix243*(4x BC) worms. n =
 618 30–45 worms per strain for each day (10–15 worms from 3 biological replicate plates).
 619 (Bottom) Calculation method of percent change in locomotor healthspan. (D) Percent
 620 change in lifespan (n = 3 biological replicate plates for WT and *ix243*(4xBC)) and
 621 locomotor healthspan (n = 3 biological replicate plates for WT and *ix243*(4xBC)) of
 622 *ix243*(4xBC) worms compared to WT. **P* < 0.05; Unpaired Student's *t* test.

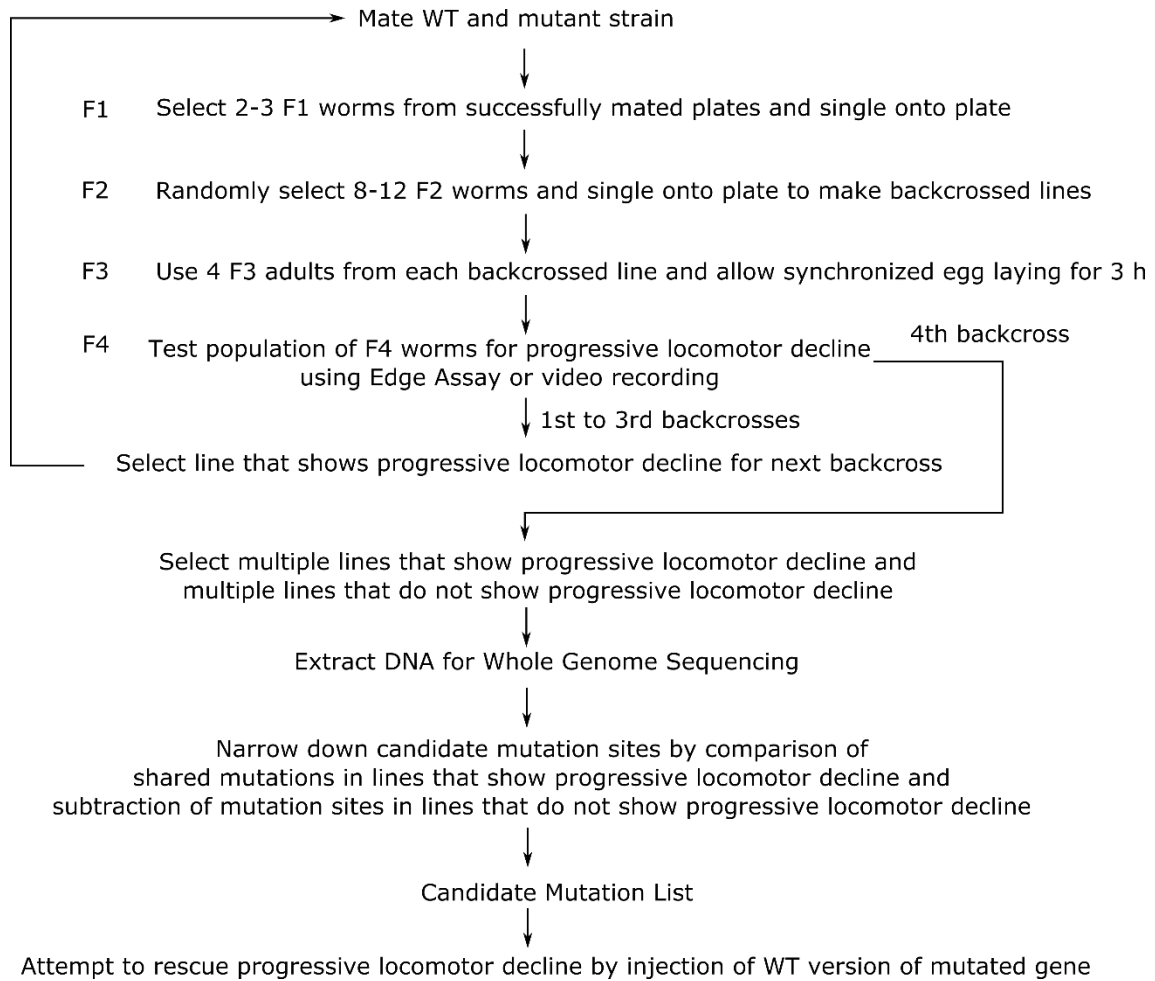
623 **Table S3. Development times of isolated mutant strains**

624 Development time from egg to first egg-lay (n=5 worms per strain).

Strain	Development Time (h)	% of WT
WT	70.4	100.0%
<i>ix239</i>	74.4	105.7%
<i>ix240</i>	71.2	101.1%
<i>ix241</i> (4x backcrossed)	73.2	104.0%
<i>ix242</i>	71.8	102.0%
<i>ix243</i> (4x backcrossed)	80.2	113.9%

625

626



627

628 **Figure S5. Strategy to identify causative mutation site**

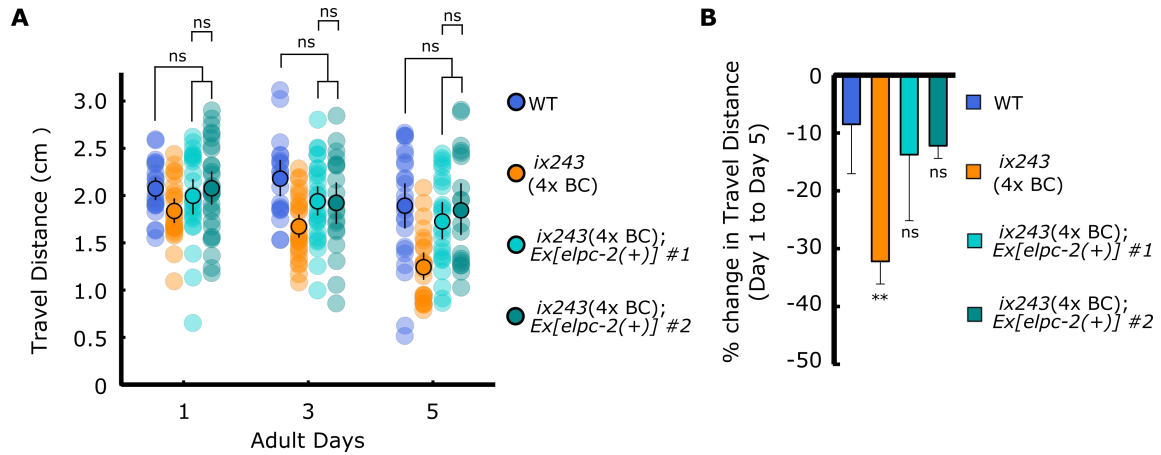
629

630 **Table S4. Remaining mutations in *ix243* mutant strains**

Chrom.	Pos.	Ref.	Alt.	Gene	Mutation Type	Effect
I	3428548	A	AGGCAGACCTAGCCCACCCTG GGCAGACCTAGCCCACCCTG	K03E5.2	downstream gene variant	modifier
I	14448378	G	GCGTCCGGTTTTGGGGTAGGTTT CCACGGCGGCCGACAATTTCCG AGTTTCGCCACTCACTATACTTA ATCAGCAATTTTATAGTGAGTTG CGAAACTCGGAAATTGTCGGCC GTCGTGGATAACTACCCCAAAA CCGGACGACCGGA	Y105E8A.27	downstream gene variant	modifier
II	1465622	C	T	Y51H7C.13	missense variant	moderate
II	1602489	C	T	bath-47	downstream gene variant	modifier
II	1717193	C	T	btb-7	downstream gene variant	modifier
II	1915528	C	T	math-31	upstream gene variant	modifier
II	2339259	G	T	F43C11.6	upstream gene variant	modifier
II	2428896	C	T	F42G2.2	downstream gene variant	modifier
II	2477652	T	A	tsr-1	upstream gene variant	modifier
II	8975684	G	T	tomm-40	upstream gene variant	modifier
III	577387	T	TAAAAATTT AACAAAA	Y55B1AL.1	downstream gene variant	modifier
III	1704981	A	T	Y22D7AR.10	upstream gene variant	modifier
III	7406703	A	T	linc-165	upstream gene variant	modifier
III	7439448	C	T	linc-165-ah-12	intergenic region	modifier
III	11024784	G	A	Y48A6B.16	upstream gene variant	modifier
III	11416475	G	A	Y47D3B.13	upstream gene variant	modifier
III	11549303	G	A	Y66D12A.14	downstream gene variant	modifier
III	11816202	G	A	C18D11.1	upstream gene variant	modifier
III	11895783	G	A	faah-5	upstream gene variant	modifier
III	12134837	G	A	Y75B8A.6	upstream gene variant	modifier
III	12156042	G	A	linc-87	upstream gene variant	modifier
III	12190456	G	A	Y75B8A.54	upstream gene variant	modifier
III	12200963	G	A	Y75B8A.44	downstream gene variant	modifier
III	12223827	G	A	Y75B8A.16	missense variant	moderate
III	12407309	G	A	tat-1	missense variant	moderate
III	12427755	G	A	Y49E10.16	upstream gene variant	modifier
III	12476529	G	A	Y49E10.33	upstream gene variant	modifier
III	12498064	C	T	Y111B2A.3	synonymous variant	low
III	12678743	G	A	elpc-2	stop gained	high
III	12701690	G	A	spin-4	downstream gene variant	modifier
III	12750669	A	T	irld-60	missense variant	moderate
III	12810002	G	A	BE10.5	upstream gene variant	modifier
III	12838123	G	A	Y37D8A.4	synonymous variant	low
III	12892115	G	A	unc-71	upstream gene variant	modifier
III	12923518	G	A	Y37D8A.16	upstream gene variant	modifier
III	12924071	G	A	mrps-10	upstream gene variant	modifier
III	13352002	G	A	F53A2.9	downstream gene variant	modifier
III	13453318	G	A	cua-1	upstream gene variant	modifier
III	13578898	G	A	T05D4.5	upstream gene variant	modifier
IV	6722231	C	T	Y73B6A.6- Y73B6A.2	intergenic region	modifier
IV	7597770	G	A	tag-80	synonymous variant	low
IV	7597783	T	A	tag-80	missense variant	moderate
IV	17276360	A	AT	ghn-5	upstream gene variant	modifier

631

632

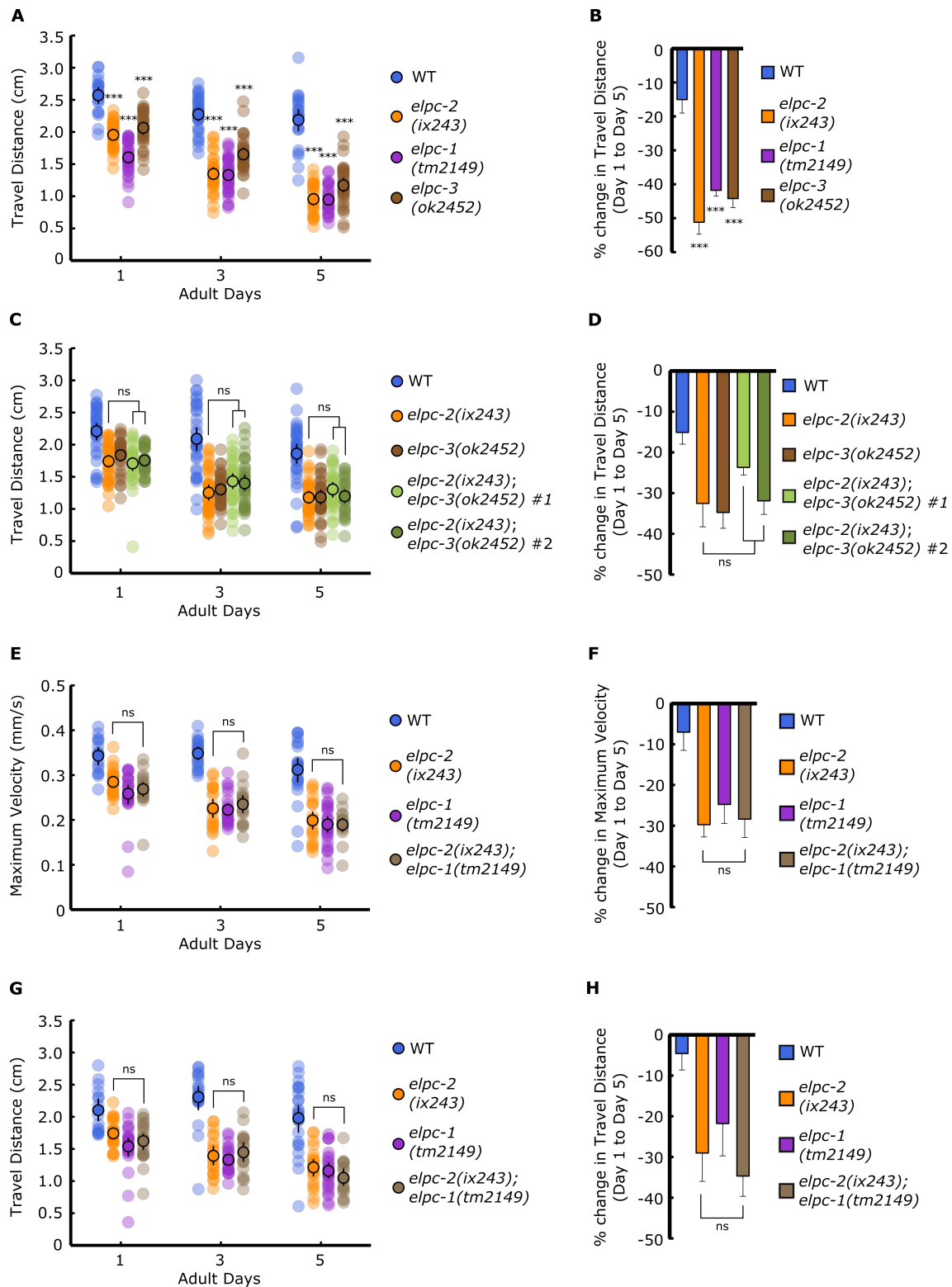


633

634 **Figure S6. Wild-type *elpc-2* gene rescues progressive decline in locomotor function**
635 **of the *ix243* mutant strain**

636 (A) Travel distance of WT, *ix243*(4x BC), *ix243*(4x BC);*Ex[elpc-2(+)]* #1, and *ix243*(4x
637 BC);*Ex[elpc-2(+)]* #2 worms. n = 30–45 worms per strain for each day (10–15 worms
638 from 3 biological replicate plates). (B) Percent change in travel distance of worms from
639 A. n = 3 biological replicate plates. ***P* < 0.01; ****P* < 0.001; ns, not significant; One-
640 way ANOVA with Dunnett's post hoc test vs. WT.

641

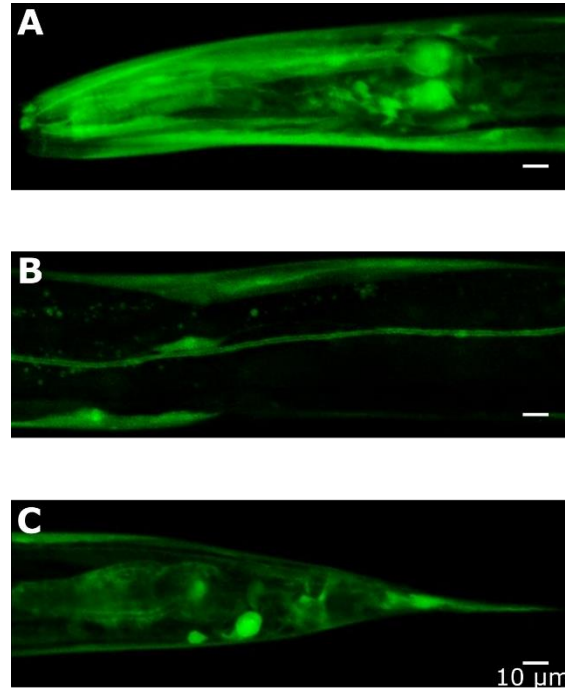


642

643 **Figure S7. The Elongator complex is required to maintain adult locomotor function**

644 (A) Travel distances of WT, *elpc-1(tm2149)* and *elpc-3(ok2452)* worms. (B) Percent
 645 change in travel distance of worms from A. (C) Travel distances of WT, *elpc-2(ix243)*,
 646 *elpc-3(ok2452)*, and *elpc-2(ix243); elpc-3(ok2452)* worms. (D) Percent change in travel
 647 distance of worms from C. (E) Maximum velocities of WT, *elpc-2(ix243)*, *elpc-1(tm2149)*,
 648 and *elpc-1(tm2149); elpc-2(ix243)* worms. (F) Percent change in maximum velocity of

649 worms from E. (G) Travel distances of WT, *elpc-2(ix243)*, *elpc-1(tm2149)*, and *elpc-*
650 *1(tm2149);elpc-2(ix243)* worms. (H) Percent change in travel distance of strains from G.
651 For maximum velocity and travel distance experiments, n = 30–45 worms per strain for
652 each day (10–15 worms from 3 biological replicate plates). For percent change in
653 maximum velocity graphs, n = 3 biological replicate plates. *** $P < 0.001$; ns, not
654 significant; One-way ANOVA with Dunnett's post hoc test vs. WT for A, B; One-way
655 ANOVA with Tukey's post hoc test for C–H.
656



657

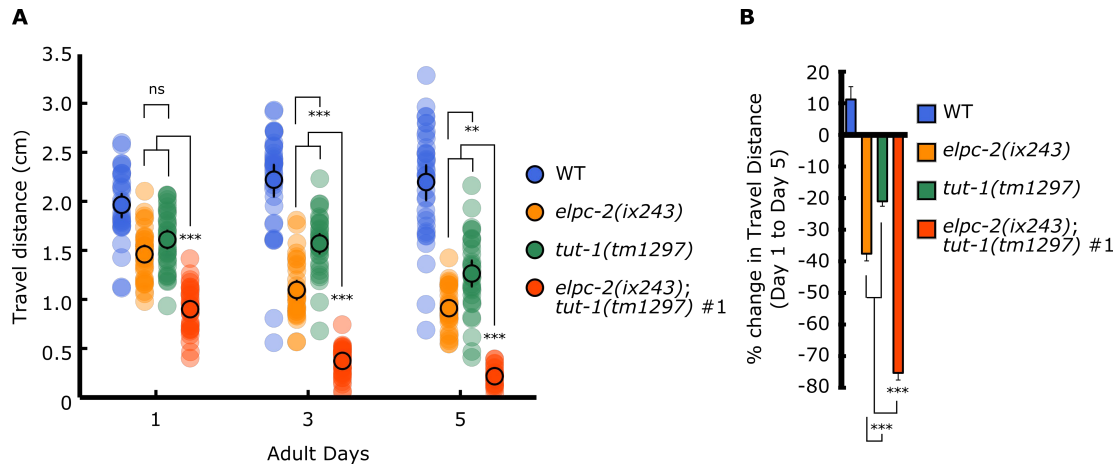
658 **Figure S8. Expression pattern of *elpc-2* transcriptional GFP fusion**

659 (A) *elpc-2p::GFP* expression in pharynx, neurons, and head muscles. (B) *elpc-2p::GFP*

660 expression in body wall muscles and canal cell. (C) *elpc-2p::GFP* expression in

661 coelomocytes, intestine, and tail. Scale bars: 10 µm.

662



663

664 **Figure S9. *tut-1(tm1297)* mutant shows progressive decline in locomotor function**

665 (A) Travel distances of WT, *elpc-2(ix243)*, *tut-1(tm1297)*, and *elpc-2(ix243);tut-*
666 *1(tm1297)* worms. n = 30–45 worms per strain for each day (10–15 worms from 3
667 biological replicate plates). (B) Percent change in travel distance of worms from A. Error
668 bars indicate 95% confidence intervals. n = 3 biological replicate plates. * $P < 0.05$; ** P
669 < 0.01 ; *** $P < 0.001$; ns, not significant; One-way ANOVA with Tukey's post hoc test.

670

671 **Table S5. Development times of *tut-1(tm1297)* and *elpc-2(ix243);tut-1(tm1297)***
672 **mutants**

673 Development time from egg to first egg-lay (n = 5 worms per strain).

Strain	Development Time (h)	% of WT
WT	70.4	100.0%
<i>tut-1(tm1297)</i>	82.0	116.5%
<i>elpc-2(ix243);tut-1(tm1297)</i>	145.4	206.5%

674

675

Q6IA86	ELP2_HUMAN	1	-----NIVPVLETSIVF-CENRNRVGLNWSGPRGLAFGTSCSVVLYD-FLKRVV	51
Q9NEW7	Q9NEW7_CAEEEL	1	MKIEEFISASVNPESHCLTAK-----TAPLVAYASSLOIAVQTIKODSEV	48
			:*:	
Q6IA86	ELP2_HUMAN	52	----TINLNGHTARVNCIOWICIKODGSPSTELVSGGSDNOVTHNEIEDNOLLKAVHLOGH	106
Q9NEW7	Q9NEW7_CAEEEL	49	GVIKSTISERRHOKPIITVL-KRLKSSSEIVADEFVTGGVDSRWVLLKLRGEHVYVADLTGC	107
			:*:	
Q6IA86	ELP2_HUMAN	107	EGPVYAVHAVYORRTSDPALCTLIISAAADSAVRLNSKKGPEVHCLOTLNFGNGFALALC	166
Q9NEW7	Q9NEW7_CAEEEL	108	DGSVGSVCGCVEDGRK--VVAAMVSETSNGFHAMVTSIGDLLNSTEIKL-DHKAFALC	164
			:*:	
Q6IA86	ELP2_HUMAN	167	LSFLPNTDVPILACGNDDCRIHFIAQ--ONDOFQKVLSCGHEDMIRGVEIAAFGRDLFL	224
Q9NEW7	Q9NEW7_CAEEEL	165	LDATSIQSVLLAVGTSKRFEVLYGESADKKSFSRLTISVAGHTDWIHSIAFNPNPDLV	224
			:*:	
Q6IA86	ELP2_HUMAN	225	ASCSDCLIRIKLYIKSTSLETO-----DDNIRLKENITETIENESVKIAFAVITL	276
Q9NEW7	Q9NEW7_CAEEEL	225	ASAGQTYVRLWAIETPEDEKSENIREDSSTTPDELTSANLESINY----TPYRCSH	280
			:*:	
Q6IA86	ELP2_HUMAN	277	TVLAGHENLVNAVHNPVYFKDGLVQPVRLLSASMDKTMILNAPDESGVHLEQVRYGE	336
Q9NEW7	Q9NEW7_CAEEEL	281	AVIQGHDDVHSTVNSND-----GRVLLTASSDKTCIINKE--IDNLRDDVRLGI	329
			:*:	
Q6IA86	ELP2_HUMAN	337	VGGN-TLGFYDCQFN-----EDGSMIIAHAFGALHLNKONTVNPREITPEIVI	384
Q9NEW7	Q9NEW7_CAEEEL	330	VGGQAGFFAAVSSSLDKDSGKIAENVVSSYFGLHCNKSTDEKTFNLTALPHT	389
			:*:	
Q6IA86	ELP2_HUMAN	385	SGHFDGVODLVNDP----EGEFTIITVGTDOTTRLFAPWKRKQDSQVTHHEIARPOIHGYD	440
Q9NEW7	Q9NEW7_CAEEEL	390	GGHVGVEVRVDWHRSDDGSGLMSVGDOTTRVFAKNG----RQSYVEIARPOVHGHD	445
			:*:	
Q6IA86	ELP2_HUMAN	441	LKCLAMINRFQFVSGADEKVLRFESAPRNVEVFCALITQSLNHVLCNODSLPEGATVP	500
Q9NEW7	Q9NEW7_CAEEEL	446	MOCLSFVNPISIFVSGAEKVFRAFRAPKSFVKSLAISQVPTKESFGSD-LAEFGACVP	504
			:*:	
Q6IA86	ELP2_HUMAN	501	ALGLSNKAVFOGDIASQPSDEEELLTSTGFEYQVAFQPSILTEPPTDHLQNTLWPEV	560
Q9NEW7	Q9NEW7_CAEEEL	505	ALGLSNKPMVEGETVDGE-----HNEEDAFRAARVVLTSPTDITLQNTLWPEQ	554
			:*:	
Q6IA86	ELP2_HUMAN	561	OKLYGHGYEIFCVTICNSKTLASACKAAKKEHAAIILNNTTSNKQVONLVFHS-LTVTQ	620
Q9NEW7	Q9NEW7_CAEEEL	555	HKLYGHGYEYVAVTANPTIGVILATACKSSHVEHSVVLNLSMNSKSEIIGHQLTVTQI	614
			:*:	
Q6IA86	ELP2_HUMAN	621	AFSPNEKFLLAVERDRTWLNKQODTISPEFEPVSLFAFTNKITSVHSRIIWSCDWSPD	680
Q9NEW7	Q9NEW7_CAEEEL	615	ANPSPGTRLLTVSRDRTAKLYTEKNGEVDGFDYD----CVWTSGRQHTRIIWACDWIDD	669
			:*:	
Q6IA86	ELP2_HUMAN	681	SKYFFITGSRDKKVVVWGECDSTDDCIEHNIGPCSSVLDVGGAVTAVSVCPLHPSORYVV	740
Q9NEW7	Q9NEW7_CAEEEL	670	EH-FVITASRQKVIVVAESAGQTAPKAT-----VKLDEPVTA-----IAAVSKDVI	714
			:*:	
Q6IA86	ELP2_HUMAN	741	AVGLECGKICLYTNKKTQVPEINDWTHCVETSQSOSHT--LAIRKLCNKNCSGKTEQKE	798
Q9NEW7	Q9NEW7_CAEEEL	715	VAGLQGTGELIVLRFDSGLH-----VIEKIGANRIPIDSAVLRIRFSKNGRK-----	761
			:*:	
Q6IA86	ELP2_HUMAN	799	AEGAENLHFA SCGEHTVYKTHRVNKCAL	826
Q9NEW7	Q9NEW7_CAEEEL	762	-----LAVATTDAKLRIFNVSQ---	778
			:*:	

676

677 **Figure S10. Amino acid alignment of *C. elegans* ELPC-2 and human ELP2**

678 *C. elegans* ELPC-2 and human ELP2 were aligned using Clustal Omega (Sievers et al.,
 679 2011). An asterisk (*) indicates positions that are conserved; colon (:) indicates positions
 680 that are strongly similar (> 0.5 in the Gonnet PAM 250 matrix); period (.) indicates
 681 positions that are weakly similar (< 0.5 in the Gonnet PAM 250 matrix).

682

683 **Supplementary Information: Strain list**

Strain	Genotype	Obtained From
CB408	<i>unc-43(e408) IV</i>	CGC
CB190	<i>unc-54(e190) I</i>	CGC
MT7929	<i>unc-13(e51)</i>	CGC
AM725	<i>rmIs290 [unc-54p ::Hsa-sod-1 (127X)::YFP]</i>	CGC
VC1937	<i>elpc-3(ok2452) V</i>	CGC
CF1038	<i>daf-16(mu86) I</i>	CGC
n/a	<i>elpc-1(tm2149) I</i>	National BioResource Project (Japan)
n/a	<i>tut-1(tm1297) IV</i>	National BioResource Project (Japan)
OF1260	<i>ix239</i>	This study
OF1261	<i>ix240</i>	This study
OF1262	<i>ix241</i>	This study
OF1263	<i>ix241</i> (4x backcrossed)	This study
OF1264	<i>ix242</i>	This study
OF1265	<i>elpc-2(ix243) III</i>	This study
OF1266	<i>elpc-2(ix243) III</i> (4x backcrossed)	This study
OF1267	<i>elpc-2(ix243) III;ixEx244[elpc-2(+);lin-44p::RFP]</i>	This study
OF1268	<i>elpc-2(ix243) III;ixEx245[elpc-2(+);lin-44p::RFP]</i>	This study
OF1269	<i>elpc-2(ix243) III;ixEx246[lin-44p::RFP]</i>	This study
OF1270	<i>ixEx247[lin-44p::RFP]</i>	This study
OF1271	<i>elpc-1(tm2149) I;elpc-2(ix243) III</i>	This study
OF1272	<i>elpc-2(ix243) III;elpc-3(ok2454) V</i> (#1)	This study
OF1273	<i>elpc-2(ix243) III;elpc-3(ok2454) V</i> (#2)	This study
OF1289	<i>elpc-2(ix243) III;tut-1(tm1297) IV</i>	This study

684

685

686 **Supplementary Information: Primer list**

Primer Name	5'-3' Sequence
5' <i>elpc-2p</i> (2090-bp upstream)	gataagtgacatgccgctgcgtccttac
3' <i>elpc-2UTR</i> (851-bp downstream)	aagagacagcgtctgattcttgaacggta
5' <i>elpc-2</i> snp	aaatgaattttcggcacaaccccaaaaa
3' <i>elpc-2</i> snp	ttcgcgaaaactctcgtagtctgacctg
5' <i>elpc-1</i> del	gaaaagcatcgagttgtccacttgaatcac
3' <i>elpc-1</i> del	ctttcagttgaattctggcatctctcaa
5' <i>elpc-3</i> del	taatagaaccagatcgagtttggcagatg
3' <i>elpc-3</i> del	aatgcatcgtatgtggttaggcggtaaac
5' <i>elpc-2p</i> overlap ppd95.79 107-	gggtaccggtagaaaaaatgaaaatcgaagaagaatttatctctgctag
3' <i>elpc-2p</i> overlap ppd95.79 138-	agttcttctccttactcatctgggaaacattaaagatttcaatttcgc
5' ppd95.79 107-	atgagtaaaggagaagaacttttactggag
3' ppd95.79 138-	ttttctaccggtaccctccaagcaagggtc

687

688

689